



Cite this: *Polym. Chem.*, 2023, **14**, 747

Leveraging the monomer structure for high-performance chemically recyclable semiaromatic polyesters†

Hua-Zhong Fan, Xing Yang, Yan-Chen Wu, Qing Cao, Zhongzheng Cai * and Jian-Bo Zhu *

The development of inexpensive and high-performance chemically recyclable polymers serves as a promising strategy for solving the issues regarding plastic pollution. In the current work, we prepared a series of aromatic monomers (DHB-R and DHN-R, R = Me, Et) derived from aromatic hydroxy acids and epoxides. Ring-opening polymerization of these monomers afforded the semiaromatic polyesters P(DHB-R) and P(DHN-R) (R = Me, Et) with high molecular weights and narrow dispersity. Remarkably, these polymers showed high thermal stability with $335\text{ }^\circ\text{C} < T_d < 350\text{ }^\circ\text{C}$. Changing the benzene ring to a naphthalene ring on the polymer backbone led to a significant improvement in the glass transition temperature (T_g), from 49 to 100 °C. P(DHB-Me) behaved as a brittle and strong material, whereas P(DHB-Et) displayed excellent ductility with an elongation at break of $762.63 \pm 94.40\%$. More importantly, P(DHB-R) and P(DHN-R) could be effectively and selectively depolymerized into the corresponding monomers, establishing a circular plastics economy.

Received 28th November 2022,
Accepted 3rd January 2023

DOI: 10.1039/d2py01491b

rsc.li/polymers

Introduction

Since their commercial production in the mid-twentieth century, plastics have become indispensable products in our daily lives. However, the accumulation of consumed plastic products has led to critical environmental problems due to their poor degradation and recyclability.^{1–3} Extensive research focused on chemical recycling of polymers to monomers (CRM) has been devoted to enabling a circular plastics economy and sustainable development.^{4–35} In a pioneering work, poly(γ-butyrolactone) from the ring-opening polymerization (ROP) of “non-polymerizable” butyrolactone was discovered to quantitatively depolymerize into its monomer γ-butyrolactone upon being heated at 220–300 °C for one hour,^{4,36} manifesting the potential of its chemical recycling in the circular plastics economy and promoting the development of this field. However, most of the currently studied polymer systems have involved aliphatic polyesters^{37–48} and chemically recyclable aromatic polyesters have been less extensively investigated. As one of the most popular thermoplastic polyesters in our daily lives, polyethylene terephthalate (PET) has been

widely utilized in fibers, resins, and filming owing to its outstanding properties associated with the aromatic moieties on the polymer backbone.^{49,50} However, its degradation and recycling requires harsh reaction conditions and inevitably suffers from side reactions.^{51–53} Moreover, it is difficult to isolate and purify the mixed products of decomposed PET.^{54–59} Therefore, designing new chemically recyclable aromatic polyesters is essential.

In 2016, Shaver and co-workers reported the ROP of 2,3-dihydro-5H-1,4-benzodioxepin (DHB) to synthesize the analogues of PET (PDHB), which could be successfully recycled to the monomer DHB in dilute solution with the catalyst salen-Al (Fig. 1).^{60,61} However, the low thermal stability of PDHB ($T_d \sim 180\text{ }^\circ\text{C}$) limited its further application. In a following work, Makwana, Lizundia and co-workers investigated the substituent effect on the *meta*-position of benzene ring, and revealed a resulting P(R-DHB) showing an improved thermal stability, specifically with a T_d in the range of 230 to 260 °C.⁶² In 2021, the Li research group designed three constitutional isomers of benzo-thia-caprolactones with great chemical recyclability to monomers under bulk thermal conditions.⁶³ The resulting semiaromatic polyesters displayed T_d values ranging from 180 to 280 °C. In the meantime, our laboratory developed a facile one-pot synthetic method for preparing a library of benzo-thia-caprolactones with various substituents from thiosalicylic acid and epoxides as the reactants.⁶⁴ The thermal and mechanical properties of the resulting aromatic polyesters could be tai-

National Engineering Laboratory of Eco-Friendly Polymeric Materials (Sichuan), College of Chemistry, Sichuan University, Chengdu 610064, People's Republic of China. E-mail: zzcai@scu.edu.cn, jbzhu@scu.edu.cn

† Electronic supplementary information (ESI) available. See DOI: <https://doi.org/10.1039/d2py01491b>

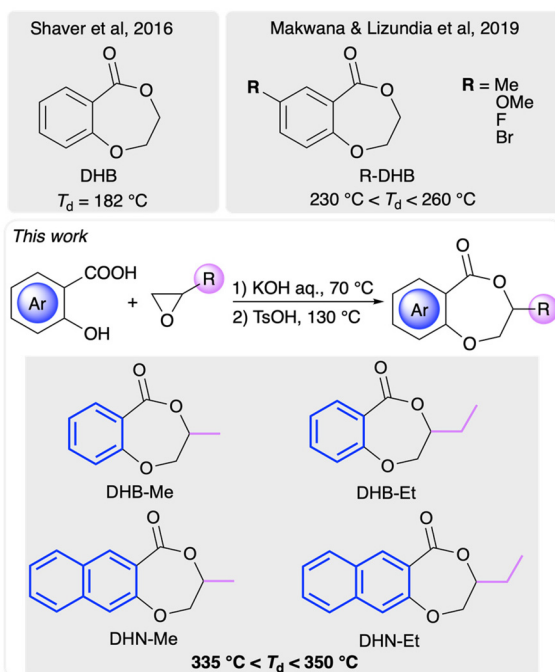


Fig. 1 Representative examples of semiaromatic monomers based on 2,3-dihydro-5H-1,4-benzodioxepin (DHB).

lored by subjecting them to functionalization and stereocomplexation to achieve high thermal stability ($285^{\circ}\text{C} < T_{\text{d}} < 310^{\circ}\text{C}$) and polyolefin-like tensile performance.

To further develop the PDHB system to meet practical applications as chemically recyclable polymers, we aimed to enhance its thermal and mechanical properties by leveraging the monomer structure. Motivated by our previous monomer design strategy based on epoxides,^{64–66} we were able to take advantage of the inexpensive and bio-derived salicylic acid and epoxides to synthesize DHB-Me and DHB-Et using a convenient two-step method. Furthermore, 3-substituted 2,3-dihydro-5H-naphthodioxepin-5-ones (DHN-R, R = Me, Et) were also prepared from 3-hydroxy-2-naphthoic acid and epoxides (Fig. 1). To our delight, these functionalized DHB/DHN-based monomers underwent efficient ROP and produced semiaromatic polyesters with excellent thermal stability ($T_{\text{d}} > 335^{\circ}\text{C}$) and tunable thermal and mechanical properties, while maintaining chemical recyclability.

Results and discussion

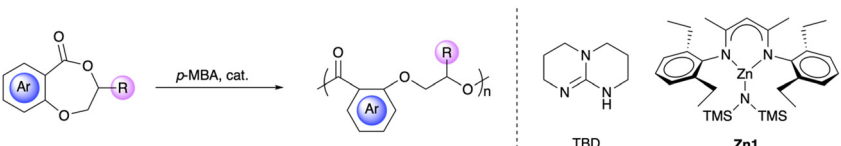
All four monomers were readily prepared on the gram scale by using a two-step synthetic route (Scheme S1†). DHB-Me and DHB-Et were synthesized from natural salicylic acid and corresponding epoxides in 46–56% overall yields. Combining the two reagents in the presence of potassium hydroxide gave an intermediate product, which underwent cyclization when treated with *p*-toluenesulfonic acid. Replacing salicylic acid with 3-hydroxy-2-naphthoic acid afforded DHN-Me and

DHN-Et in 44–65% yields. Owing to the commercial availability of enantiopure (*R*)-propylene oxide, we were able to obtain (*R*)-DHB-Me and (*R*)-DHN-Me using a similar procedure. This synthetic method can endow polymers with diverse functional groups and precise stereocenters.

As 1,5,7-triazabicyclo[4.4.0]dec-5-ene (TBD) has been reported to be an effective organocatalyst for ROP of cyclic esters,^{67–76} TBD-catalyzed ROP of monomers was first investigated in bulk conditions. The polymerization of DHB-Me with a [DHB-Me]:[TBD]:[I] ratio of 100:1:1 reached 71% conversion within 1 h at 70°C (Table 1, entry 1). As a comparison, DHB-Et with a bulkier ethyl substituent exhibited lower reactivity, approaching 69% conversion in 3 h under similar conditions (Table 1, entry 9). At an increased [monomer]:[TBD]:[I] ratio of 500:1:1, the polymerizations occurred with 76% and 60% conversions of, respectively, DHB-Me and DHB-Et in 12 h (Table 1, entries 2 and 10). The number-average molecular weights (M_{ns}) of the resulting polymers were much lower than the calculated values ($M_{\text{n, theos}}$), indicating that this TBD catalytic polymerization system was not well controlled.

To improve the polymerization efficiency of this system, the organometallic complex **Zn1**⁷⁷ was investigated as the catalyst. Gratifyingly, **Zn1** displayed improved activity for the ROPs of DHB-Me and DHB-Et with turnover frequencies (TOFs) ranging from 125 to 320 h^{-1} (Table 1, entries 3, 4, 11 and 12). Impressively, P(DHB-Et) with a high M_{n} of 123 kDa and relatively narrow dispersity of 1.17 was obtained when using a [DHB-Et]:[**Zn1**]:[I] ratio of 1000:1:1 (Table 1, entry 12). The ROPs of DHN-Me and DHN-Et were carried out with **Zn1** as a catalyst and *p*-tolylmethanol as an initiator in toluene at 100°C , due to their high melting temperatures and poor solubility levels. Monomer conversions of 64% and 52% were achieved for DHN-Me and DHN-Et at a [monomer]:[**Zn1**]:[I] ratio of 1000:1:1, demonstrating TOFs of 91.4 h^{-1} and 86.7 h^{-1} , respectively. The produced P(DHN-Me) and P(DHN-Et) showed a range of M_{ns} from 15.9 to 88.7 kDa and a relatively narrow distribution of molecular weights ($D < 1.25$). Additionally, enantiopure monomers (*R*)-DHB-Me and (*R*)-DHN-Me underwent polymerization in a similar fashion as did racemic monomers and afforded isotactic P[*(R*)-DHB-Me] and P[*(R*)-DHN-Me] with M_{ns} of 36.6 and 42.5 kg mol⁻¹, respectively (Table 1, entries 6 and 17). Their isotactic arrangements were confirmed using ¹³C NMR spectroscopy, with the observation of only one set of resonances (Fig. S19 and S27†).

The linear structure and high fidelity of *p*-methylbenzyl terminal groups of the produced polymer were evaluated using matrix-assisted laser desorption ionization time-of-flight (MALDI-TOF) mass spectrometry (Fig. S34†). The MALDI-TOF mass spectrum of a P(DHB-Me) sample prepared from a 50:1:1 ratio of [DHB-Me]:[**Zn1**]:[I] displayed a series of molecular ion peaks showing a neighboring spacing of 178.38, which was consistent with the molar mass of the DHB-Me repeat unit. The intercept of a line fitted to the data was found to be 145.17, matching the total mass of chain ends plus the mass of Na^+ [$M_{\text{end}} = 122.17 (\text{CH}_3\text{C}_6\text{H}_4\text{CH}_2\text{OH}) \text{ g mol}^{-1} + 23$]

Table 1 Polymerization of the monomers^a


Entry	Monomer	Cat.	[M]/[I]/[Cat.]	Time/h	Conv. ^b /%	$M_n, \text{theo}^c/\text{kDa}$	$M_n, \text{SEC}^d/\text{kDa}$	D^d	$T_g^e/\text{°C}$	$T_d^f/\text{°C}$
1	DHB-Me	TBD	100:1:1	1	71	12.6	9.1	1.22	—	—
2	DHB-Me	TBD	500:1:1	12	76	67.7	35.0	1.25	64	340
3	DHB-Me	Zn1	500:1:1	2	64	57.0	45.0	1.34	65	342
4	DHB-Me	Zn1	1000:1:1	6	75	134	97.6	1.19	65	343
5	(R)-DHB-Me	TBD	100:1:1	1	77	13.7	10.7	1.20	60	336
6	(R)-DHB-Me	Zn1	500:1:1	6	60	53.4	36.6	1.25	63	345
7	(S)-DHB-Me	TBD	100:1:1	1	77	13.7	10.6	1.17	58	335
8	(S)-DHB-Me	TBD	500:1:1	6	63	56.1	36.6	1.23	—	—
9	DHB-Et	TBD	100:1:1	3	69	13.2	12.4	1.20	—	—
10	DHB-Et	TBD	500:1:1	12	60	57.6	31.1	1.24	48	342
11	DHB-Et	Zn1	500:1:1	1	64	61.5	73.9	1.23	49	349
12	DHB-Et	Zn1	1000:1:1	4	68	130	123	1.17	50	339
13	DHN-Me	Zn1	100:1:1	1	74	21.3	20.0	1.25	—	—
14	DHN-Me	Zn1	500:1:1	6	66	75.3	66.0	1.13	118	336
15	DHN-Me	Zn1	1000:1:1	7	64	146	88.7	1.18	114	345
16	(R)-DHN-Me	Zn1	100:1:1	1	74	16.9	14.9	1.38	109	—
17	(R)-DHN-Me	Zn1	500:1:1	4	91	104	42.5	1.57	121	349
18	(S)-DHN-Me	Zn1	100:1:1	1	71	16.2	13.1	1.39	110	—
19	DHN-Et	Zn1	100:1:1	1	55	13.3	15.9	1.23	—	—
20	DHN-Et	Zn1	500:1:1	3	54	65.4	44.6	1.13	100	344
21	DHN-Et	Zn1	1000:1:1	6	52	126	66.7	1.10	—	—

^aThe polymerizations of DHB-Me and DHB-Et were conducted at bulk conditions, 70 °C; and the polymerizations of DHN-Me and DHN-Et were carried out in toluene solution (2 M) at 100 °C. ^bCalculated from the ¹H NMR spectrum in CDCl₃. ^c $M_n, \text{theo} = \text{MW (monomer)} \times [\text{M}]_0/[\text{I}]_0 \times \text{Conv.} + \text{MW (terminal group)}$. ^dNumber-average molecular weight (M_n) and dispersity index ($D = M_w/M_n$) determined from the results of size exclusion chromatography (SEC) performed at 40 °C in THF. ^e T_g measured from the results of differential scanning calorimetry (DSC), specifically from the second heating-scan curves with a cooling and second heating rate of 10 °C min⁻¹. ^f T_d measured from the results of thermal gravimetric analysis (TGA) carried out at a heating rate of 10 °C min⁻¹.

(Na⁺) g mol⁻¹], confirming the linear structure of CH₃C₆H₄CH₂O-[DHB-Me]_n-H.

Thermal gravimetric analysis (TGA) and differential scanning calorimetry (DSC) were utilized to assess the thermal properties of the produced polymers. All these polymers exhibited excellent thermal stability—with the onset decomposition temperature (T_d), defined as the temperature at 5% weight loss, ranging from 336 °C to 349 °C (Fig. 2a). These values were about 160 °C higher than that of P(DHB),⁶¹ highlighting the significant improvement in thermal stability resulting from including the substitutions in P(DHB).

P(DHB-Me) and P(DHB-Et) showed glass transition temperature (T_g) values of 65 °C and 49 °C, respectively. In contrast, P(DHN-Me) and P(DHN-Et) showed higher T_g values of 118 °C and 100 °C (Fig. 2b), which could be attributed to the more rigid naphthalene structures in these two polymers. The absence of a melting transition revealed the amorphous feature of these polymers. Initially, we hypothesized that the lack of crystallinity was due to their atactic structures. The thermal transitions of isotactic P[(R)-DHB-Me] and P[(S)-DHB-Me] were subsequently investigated. Surprisingly, melting

transitions were observed neither for P[(R)-DHB-Me] nor for P[(S)-DHN-Me] (Fig. S43 and S46†). Compared with the previously reported sulfur-containing systems,⁶⁴ we inferred that the heteroatoms in the system might be responsible for the crystallinity of the material. We investigated the stereocomplexation of the polymers by mixing isotactic (R)-polymer and (S)-polymer in a 1:1 molar ratio (approximately 100 mg in total). Unfortunately, no stereocomplexation was observed for either of these systems. DSC and PXRD analyses were carried out to characterize the formation of stereocomplexes (Fig. S56†). However, melting transitions were neither observed for the isotactic polymers nor for their blends. Additionally, the absence of sharp peaks for (R)-polymer, (S)-polymer, and their mixture in their PXRD patterns further confirmed the amorphous character of the polymers.

The enhanced thermal properties of these semiaromatic polyesters encouraged us to investigate their mechanical properties. Uniaxial tensile tests were performed on hot-pressed dogbone-shape films at an extension rate of 10 mm min⁻¹ (Fig. 3). P(DHB-Me) behaved as a stiff material with high tensile strength ($\sigma_B = 33.69 \pm 5.39$ MPa), Young's modulus ($E =$

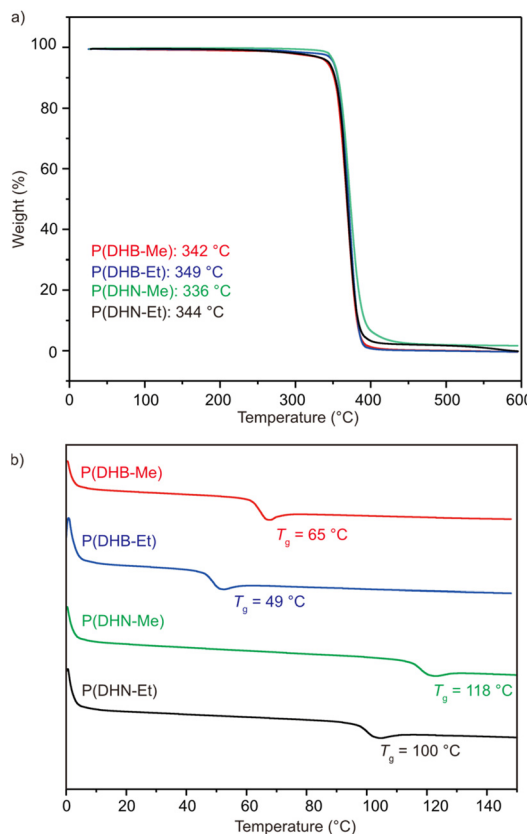


Fig. 2 Thermal properties of the produced semiaromatic polyesters. (a) TGA curves of P(DHB-Me), P(DHB-Et), P(DHN-Me), and P(DHN-Et). (b) DSC curves of P(DHB-Me), P(DHB-Et), P(DHN-Me), and P(DHN-Et).

2.17 ± 0.36 GPa), and elongation at break ($\varepsilon_B = 10.91 \pm 2.15\%$). In comparison to P(DHB-Me), the isotactic P[(R)-DHB-Me] and P[(S)-DHB-Me] displayed similar tensile performances (Table S4 and Fig. S58†). In contrast, P(DHB-Et) displayed a σ_B value of 3.16 ± 0.57 MPa and an ε_B of $762.63 \pm 94.40\%$. The distinct tensile performances of P(DHB-Me) and P(DHB-Et) manifested the profound impact of pendant groups on the mechanical properties of polymers. We hypothesized that the ethyl substituents in P(DHB-Et) were more flexible than the methyl side chain in P(DHB-Me), and that this difference in flexibility contributed to a significant difference between the packings of the polymer chains. Moreover, the T_g value of P(DHB-Et) was close to room temperature, which also led to the improved ductility of the P(DHB-Et) film measured at room temperature. P(DHN-Me) and P(DHN-Et) appeared to be brittle with an $\varepsilon_B < 5\%$ and $\sigma_B > 35$ MPa. We believe that the strength and brittleness of these polymers were due to the rigidity of their naphthalene moieties. Interestingly, attempts to improve the ductility of P(DHB-Me) via copolymerization with DHB-Et was unsuccessful. A copolymer P(DHB-Me-*co*-DHB-Et) with only 7 mol% DHB-Me was prepared by carrying out a one-pot copolymerization of DHB-Me and DHB-Et in a [DHB-Me]:[DHB-Et]:[Zn1]:[I] feed ratio of 50:1000:1:1

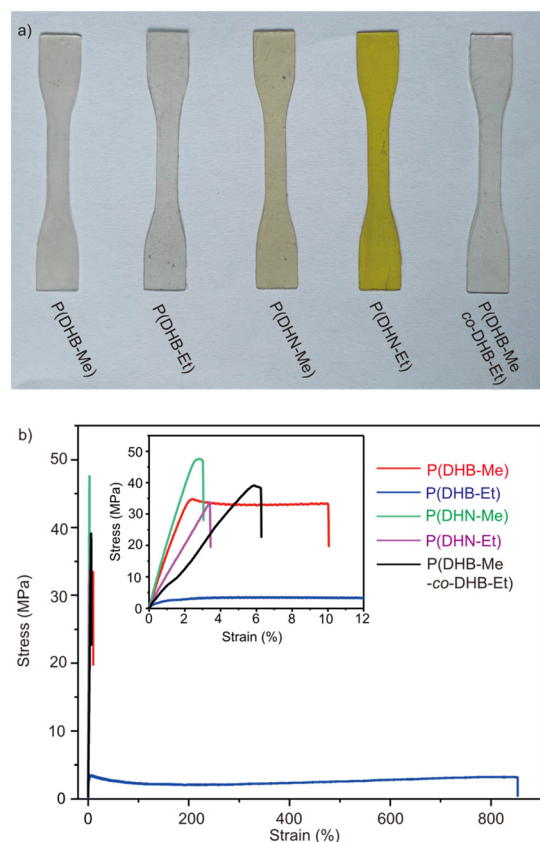


Fig. 3 (a) Images of the polymer films used for the tensile test. (b) Stress-strain curves of the produced polymers.

(with the composition determined from ^1H NMR analysis, Fig. S32†). This P(DHB-Me-*co*-DHB-Et) copolymer ($M_n = 57.5$ kDa, $D = 1.13$) performed as a hard and tough material like P(DHB-Me) with $\sigma_B = 38.16 \pm 3.56$ MPa and $\varepsilon_B = 5.86 \pm 0.65\%$.

Prior to performing the chemical recycling study, we investigated the thermodynamics of the ROP of DHB-Me at $[\text{DHB-Me}]_0 = 2$ M (Fig. S63†). The thermodynamic parameters ΔH_p° and ΔS_p° were calculated to be -14.8 kJ mol $^{-1}$ and -43.3 J mol $^{-1}$ K $^{-1}$, respectively. The ceiling temperature T_c at an initial monomer concentration of 1 mol L $^{-1}$ was determined to be 69 °C according to the equation $T_c = \Delta H_p^\circ / (\Delta S_p^\circ + R \ln [\text{M}]_0)$, indicative of excellent recyclability. Chemical recycling to monomers of these synthesized polymers were next tested in dilute solution. With 5 mol% Zn1 loading, the depolymerizations of P(DHB-Me) and P(DHB-Et) underwent nearly quantitative conversions to DHB-Me and DHB-Et in 30 minutes at 120 °C (Fig. 4 and Fig. S64†), while P(DHN-Me) and P(DHN-Et) showed moderately lower yields of 80% and 83% at 140 °C (Fig. S65 and S66†). When 10 mol% TBD was used as a catalyst, DHN-Me and DHN-Et were selectively recycled with high conversions of 93% and 98%, respectively (Table S10†). These results demonstrated a high efficiency for the chemical recycling of these synthesized polymers.

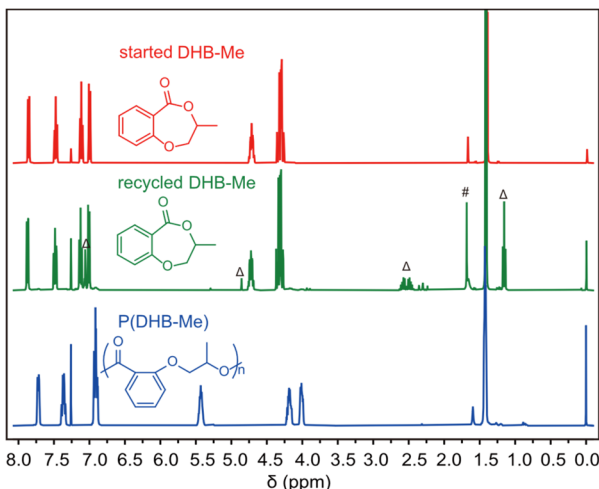


Fig. 4 ^1H NMR spectra of chemical recycling study of P(DHB-Me) (Δ , residual Zn1 catalyst; #, H_2O).

Conclusions

In summary, we have reported a facile synthetic route to prepare functionalized DHB-based monomers from aromatic hydroxy acids and epoxides. These monomers underwent efficient polymerization and afforded semiaromatic polyesters with high M_n values and narrow dispersity. Importantly, all these polymer products demonstrated high thermal stability with $T_d > 335$ °C. The introduction of naphthalene groups into the polymer main chain enhanced the T_g values of P(DHN-R) significantly ($T_g > 100$ °C). Interestingly, P(DHB-Et) performed as a flexible material with an ϵ_B of $762.63 \pm 94.40\%$, while P(DHB-Me) appeared to be strong and brittle with $\sigma_B = 33.69 \pm 5.39$ MPa, $E = 2.17 \pm 0.36$ Gpa, and $\epsilon_B = 10.91 \pm 2.15\%$ —indicative of the potential applications of these polymers, from elastomers to thermoplastics. We also found that the produced polymers could be efficiently recycled, *i.e.*, converted back to their corresponding monomers with high yields. This functionalization method involving introducing epoxide building blocks into the PDHB system was also found to strongly modulate the thermal and mechanical properties of the materials.

Conflicts of interest

The authors declare no conflict of interest.

Acknowledgements

This work was supported by the National Natural Science Foundation of China (51903177 and 22071163), the “1000 Youth Talents Program”, and the Fundamental Research Funds for the Central Universities (YJ201924 and YJ202209).

References

- 1 S. B. Borrelle, J. Ringma, K. L. Law, C. C. Monnahan, L. Lebreton, A. McGivern, E. Murphy, J. Jambeck, G. H. Leonard, M. A. Hilleary, M. Eriksen, H. P. Possingham, H. De Frond, L. R. Gerber, B. Polidoro, A. Tahir, M. Bernard, N. Mallos, M. Barnes and C. M. Rochman, *Science*, 2020, **369**, 1515–1518.
- 2 M. MacLeod, H. P. H. Arp, M. B. Tekman and A. Jahnke, *Science*, 2021, **373**, 61–65.
- 3 R. Geyer, in *Plastic Waste and Recycling*, ed. T. M. Letcher, Academic Press, 2020, pp. 13–32, DOI: [10.1016/B978-0-12-817880-5.00002-5](https://doi.org/10.1016/B978-0-12-817880-5.00002-5).
- 4 M. Hong and E. Y. X. Chen, *Nat. Chem.*, 2016, **8**, 42–49.
- 5 J.-B. Zhu, E. M. Watson, J. Tang and E. Y. X. Chen, *Science*, 2018, **360**, 398–403.
- 6 B. A. Abel, R. L. Snyder and G. W. Coates, *Science*, 2021, **373**, 783–789.
- 7 Y.-M. Tu, X.-M. Wang, X. Yang, H.-Z. Fan, F.-L. Gong, Z. Cai and J.-B. Zhu, *J. Am. Chem. Soc.*, 2021, **143**, 20591–20597.
- 8 Y. Liu, H. Zhou, J.-Z. Guo, W.-M. Ren and X.-B. Lu, *Angew. Chem., Int. Ed.*, 2017, **56**, 4862–4866.
- 9 W. C. Ellis, Y. Jung, M. Mulzer, R. Di Girolamo, E. B. Lobkovsky and G. W. Coates, *Chem. Sci.*, 2014, **5**, 4004–4011.
- 10 D. J. Saxon, E. A. Gormong, V. M. Shah and T. M. Reineke, *ACS Macro Lett.*, 2021, **10**, 98–103.
- 11 J. P. Lutz, O. Davydovich, M. D. Hannigan, J. S. Moore, P. M. Zimmerman and A. J. McNeil, *J. Am. Chem. Soc.*, 2019, **141**, 14544–14548.
- 12 Y. Liu, Y. Jia, Q. Wu and J. S. Moore, *J. Am. Chem. Soc.*, 2019, **141**, 17075–17080.
- 13 P. R. Christensen, A. M. Scheuermann, K. E. Loeffler and B. A. Helms, *Nat. Chem.*, 2019, **11**, 442–448.
- 14 C. Shi, M. L. McGraw, Z.-C. Li, L. Cavallo, L. Falivene and E. Y. X. Chen, *Sci. Adv.*, 2020, **6**, eabc0495.
- 15 D. Sathe, J. Zhou, H. Chen, H.-W. Su, W. Xie, T.-G. Hsu, B. R. Schrage, T. Smith, C. J. Ziegler and J. Wang, *Nat. Chem.*, 2021, **13**, 743–750.
- 16 K. A. Stellmach, M. K. Paul, M. Xu, Y.-L. Su, L. Fu, A. R. Toland, H. Tran, L. Chen, R. Ramprasad and W. R. Gutekunst, *ACS Macro Lett.*, 2022, **11**, 895–901.
- 17 R. M. Cywar, N. A. Rorrer, H. B. Mayes, A. K. Maurya, C. J. Tassone, G. T. Beckham and E. Y. X. Chen, *J. Am. Chem. Soc.*, 2022, **144**, 5366–5376.
- 18 J. Yuan, W. Xiong, X. Zhou, Y. Zhang, D. Shi, Z. Li and H. Lu, *J. Am. Chem. Soc.*, 2019, **141**, 4928–4935.
- 19 W. Xiong, W. Chang, D. Shi, L. Yang, Z. Tian, H. Wang, Z. Zhang, X. Zhou, E.-Q. Chen and H. Lu, *Chem.*, 2020, **6**, 1831–1843.
- 20 H. S. Wang, N. P. Truong, Z. Pei, M. L. Coote and A. Anastasaki, *J. Am. Chem. Soc.*, 2022, **144**, 4678–4684.
- 21 Y.-T. Guo, C. Shi, T.-Y. Du, X.-Y. Cheng, F.-S. Du and Z.-C. Li, *Macromolecules*, 2022, **55**, 4000–4010.

22 M. Mohadjer Beromi, C. R. Kennedy, J. M. Younker, A. E. Carpenter, S. J. Mattler, J. A. Throckmorton and P. J. Chirik, *Nat. Chem.*, 2021, **13**, 156–162.

23 J. D. Feist and Y. Xia, *J. Am. Chem. Soc.*, 2020, **142**, 1186–1189.

24 J.-Z. Zhao, T.-J. Yue, B.-H. Ren, Y. Liu, W.-M. Ren and X.-B. Lu, *Macromolecules*, 2022, **55**, 8651–8658.

25 Y. Wang, M. Li, J. Chen, Y. Tao and X. Wang, *Angew. Chem., Int. Ed.*, 2021, **60**, 22547–22553.

26 G.-Q. Tian, Z.-H. Yang, W. Zhang, S.-C. Chen, L. Chen, G. Wu and Y.-Z. Wang, *Green Chem.*, 2022, **24**, 4490–4497.

27 Q. Zhang, Y. Deng, C.-Y. Shi, B. L. Feringa, H. Tian and D.-H. Qu, *Matter*, 2021, **4**, 1352–1364.

28 G.-W. Yang, Y. Wang, H. Qi, Y.-Y. Zhang, X.-F. Zhu, C. Lu, L. Yang and G.-P. Wu, *Angew. Chem., Int. Ed.*, 2022, **61**, e202210243.

29 T. M. McGuire, A. C. Deacy, A. Buchard and C. K. Williams, *J. Am. Chem. Soc.*, 2022, **144**, 18444–18449.

30 X. Liao, F.-C. Cui, J.-H. He, W.-M. Ren, X.-B. Lu and Y.-T. Zhang, *Chem. Sci.*, 2022, **13**, 6283–6290.

31 C. Li, R. J. Sablong, R. A. T. M. van Benthem and C. E. Koning, *ACS Macro Lett.*, 2017, **6**, 684–688.

32 Z. Cai, Y. Liu, Y.-H. Tao and J.-B. Zhu, *Acta Chim. Sin.*, 2022, **80**, 1165–1182.

33 W. Zhang, J. Dai, Y.-C. Wu, J.-X. Chen, S.-Y. Shan, Z. Cai and J.-B. Zhu, *ACS Macro Lett.*, 2022, **11**, 173–178.

34 G. W. Coates and Y. D. Y. L. Getzler, *Nat. Rev. Mater.*, 2020, **5**, 501–516.

35 Y. Yu, B. Gao, Y. Liu and X.-B. Lu, *Angew. Chem., Int. Ed.*, 2022, **61**, e202204492.

36 M. Hong and E. Y. X. Chen, *Angew. Chem., Int. Ed.*, 2016, **55**, 4188–4193.

37 L. Cederholm, P. Olsén, M. Hakkarainen and K. Odelius, *Polym. Chem.*, 2020, **11**, 4883–4894.

38 G. W. Fahnhorst and T. R. Hoye, *ACS Macro Lett.*, 2018, **7**, 143–147.

39 J. Li, F. Liu, Y. Liu, Y. Shen and Z. Li, *Angew. Chem., Int. Ed.*, 2022, **61**, e202207105.

40 C. Li, L. Wang, Q. Yan, F. Liu, Y. Shen and Z. Li, *Angew. Chem., Int. Ed.*, 2022, **61**, e202201407.

41 X. Tang and E. Y. X. Chen, *Chem.*, 2019, **5**, 284–312.

42 X.-L. Li, R. W. Clarke, J.-Y. Jiang, T.-Q. Xu and E. Y. X. Chen, *Nat. Chem.*, 2022, DOI: [10.1038/s41557-022-01077-x](https://doi.org/10.1038/s41557-022-01077-x).

43 J. Su, G. Xu, B. Dong, R. Yang, H. Sun and Q. Wang, *Polym. Chem.*, 2022, **13**, 5897–5904.

44 R. M. Rapagnani, R. J. Dunscomb, A. A. Fresh and I. A. Tonks, *Nat. Chem.*, 2022, **14**, 877–883.

45 L. Cederholm, J. Wohlert, P. Olsén, M. Hakkarainen and K. Odelius, *Angew. Chem., Int. Ed.*, 2022, **61**, e202204531.

46 J. Bruckmoser, S. Remke and B. Rieger, *ACS Macro Lett.*, 2022, **11**, 1162–1166.

47 D. K. Schneiderman, M. E. Vanderlaan, A. M. Mannion, T. R. Panthani, D. C. Batiste, J. Z. Wang, F. S. Bates, C. W. Macosko and M. A. Hillmyer, *ACS Macro Lett.*, 2016, **5**, 515–518.

48 J. Dai, W. Xiong, M.-R. Du, G. Wu, Z. Cai and J.-B. Zhu, *Sci. China: Chem.*, 2023, **66**, 251–258.

49 M. Niaounakis, in *Recycling of Flexible Plastic Packaging*, ed. M. Niaounakis, William Andrew Publishing, 2020, pp. 1–20, DOI: [10.1016/B978-0-12-816335-1.00001-3](https://doi.org/10.1016/B978-0-12-816335-1.00001-3).

50 J. C. C. Yeo, J. K. Muiruri, W. Thitsartarn, Z. Li and C. He, *Mater. Sci. Eng., C*, 2018, **92**, 1092–1116.

51 S. W. Lee, M. Ree, C. E. Park, Y. K. Jung, C. S. Park, Y. S. Jin and D. C. Bae, *Polymer*, 1999, **40**, 7137–7146.

52 D. A. Schiraldi, in *Modern Polyesters: Chemistry and Technology of Polyesters and Copolyesters*, 2004, pp. 243–265, DOI: [10.1002/0470090685.ch6](https://doi.org/10.1002/0470090685.ch6).

53 F. Zhang, F. Wang, X. Wei, Y. Yang, S. Xu, D. Deng and Y.-Z. Wang, *J. Energy Chem.*, 2022, **69**, 369–388.

54 H. Wang, Z. Li, Y. Liu, X. Zhang and S. Zhang, *Green Chem.*, 2009, **11**, 1568–1575.

55 Q. Wang, X. Yao, S. Tang, X. Lu, X. Zhang and S. Zhang, *Green Chem.*, 2012, **14**, 2559–2566.

56 K. Fukushima, J. M. Lecuyer, D. S. Wei, H. W. Horn, G. O. Jones, H. A. Al-Megren, A. M. Alabdulrahman, F. D. Alsewailem, M. A. McNeil, J. E. Rice and J. L. Hedrick, *Polym. Chem.*, 2013, **4**, 1610–1616.

57 C. Jehanno, I. Flores, A. P. Dove, A. J. Müller, F. Ruipérez and H. Sardon, *Green Chem.*, 2018, **20**, 1205–1212.

58 C. S. Nunes, M. J. Vieira da Silva, D. Cristina da Silva, A. d. R. Freitas, F. A. Rosa, A. F. Rubira and E. C. Muniz, *RSC Adv.*, 2014, **4**, 20308–20316.

59 C. Jehanno, J. Demarteau, D. Mantione, M. C. Arno, F. Ruipérez, J. L. Hedrick, A. P. Dove and H. Sardon, *Angew. Chem., Int. Ed.*, 2021, **60**, 6710–6717.

60 J. P. MacDonald and M. P. Shaver, *Polym. Chem.*, 2016, **7**, 553–559.

61 E. Lizundia, V. A. Makwana, A. Larrañaga, J. L. Vilas and M. P. Shaver, *Polym. Chem.*, 2017, **8**, 3530–3538.

62 V. A. Makwana, A. Larrañaga, J. L. Vilas and E. Lizundia, *Polym. Degrad. Stab.*, 2019, **169**, 108984.

63 L.-G. Li, Q.-Y. Wang, Q.-Y. Zheng, F.-S. Du and Z.-C. Li, *Macromolecules*, 2021, **54**, 6745–6752.

64 H.-Z. Fan, X. Yang, J.-H. Chen, Y.-M. Tu, Z. Cai and J.-B. Zhu, *Angew. Chem., Int. Ed.*, 2022, **61**, e202117639.

65 X. Yang, W. Zhang, H.-Y. Huang, J. Dai, M.-Y. Wang, H.-Z. Fan, Z. Cai, Q. Zhang and J.-B. Zhu, *Macromolecules*, 2022, **55**, 2777–2786.

66 X. Yang, H.-Z. Fan, Z. Cai, Q. Zhang and J.-B. Zhu, *Chin. J. Chem.*, 2022, **40**, 2973–2980.

67 R. C. Pratt, B. G. G. Lohmeijer, D. A. Long, R. M. Waymouth and J. L. Hedrick, *J. Am. Chem. Soc.*, 2006, **128**, 4556–4557.

68 L. Simón and J. M. Goodman, *J. Org. Chem.*, 2007, **72**, 9656–9662.

69 B. G. G. Lohmeijer, R. C. Pratt, F. Leibfarth, J. W. Logan, D. A. Long, A. P. Dove, F. Nederberg, J. Choi, C. Wade, R. M. Waymouth and J. L. Hedrick, *Macromolecules*, 2006, **39**, 8574–8583.

70 X. Sun, J. P. Gao and Z. Y. Wang, *J. Am. Chem. Soc.*, 2008, **130**, 8130–8131.

71 R. Todd, S. Tempelaar, G. Lo Re, S. Spinella, S. A. McCallum, R. A. Gross, J.-M. Raquez and P. Dubois, *ACS Macro Lett.*, 2015, **4**, 408–411.

72 S. Moins, C. Henoumont, J. De Winter, A. Khalil, S. Laurent, S. Cammas-Marion and O. Coulembier, *Polym. Chem.*, 2018, **9**, 1840–1847.

73 R. M. Shakaroun, P. Jéhan, A. Alaaeddine, J.-F. Carpentier and S. M. Guillaume, *Polym. Chem.*, 2020, **11**, 2640–2652.

74 A. Pascual, H. Sardon, A. Veloso, F. Ruipérez and D. Mecerreyres, *ACS Macro Lett.*, 2014, **3**, 849–853.

75 Y.-T. Guo, W. Xiong, C. Shi, F.-S. Du and Z.-C. Li, *Polym. Chem.*, 2022, **13**, 4490–4501.

76 D. Ragno, G. Di Carmine, M. Vannini, O. Bortolini, D. Perrone, S. Buoso, M. Bertoldo and A. Massi, *Polym. Chem.*, 2022, **13**, 1350–1358.

77 M. Cheng, A. B. Attygalle, E. B. Lobkovsky and G. W. Coates, *J. Am. Chem. Soc.*, 1999, **121**, 11583–11584.